Received: 27 April 2020 | Revised: 7 July 2020 | Accepted: 13 July 2020

DOI: 10.1111/ina.12720

ORIGINAL ARTICLE

WILEY

Could the ductless personalized ventilation be an alternative to the regular ducted personalized ventilation?

Hayder Alsaad | Conrad Voelker

Department of Building Physics, Bauhaus-Universität Weimar, Weimar, Germany

Correspondence
Hayder Alsaad, Department of Building Physics, Bauhaus-Universität Weimar, Coudraystrasse 11A, 99423 Weimar, Germany.
Email: hayder.alsaad@uni-weimar.de

Funding information
Deutscher Akademischer Austauschdienst, Grant/Award Number: Programme ID: 57129429.; Open access funding enabled and organized by Projekt DEAL

Abstract

This study investigates the performance of two systems: personalized ventilation (PV) and ductless personalized ventilation (DPV). Even though the literature indicates a compelling performance of PV, it is not often used in practice due to its impracticality. Therefore, the present study assesses the possibility of replacing the inflexible PV with DPV in office rooms equipped with displacement ventilation (DV) in the summer season. Numerical simulations were utilized to evaluate the inhaled concentration of pollutants when PV and DPV are used. The systems were compared in a simulated office with two occupants: a susceptible occupant and a source occupant. Three types of pollution were simulated: exhaled infectious air, dermally emitted contamination, and room contamination from a passive source. Results indicated that PV improved the inhaled air quality regardless of the location of the pollution source; a higher PV supply flow rate positively impacted the inhaled air quality. Contrarily, the performance of DPV was highly sensitive to the source location and the personalized flow rate. A higher DPV flow rate tends to decrease the inhaled air quality due to increased mixing of pollutants in the room. Moreover, both systems achieved better results when the personalized system of the source occupant was switched off.

KEYWORDS

computational fluid dynamics, cross-contamination, ductless personalized ventilation, indoor air quality, personalized ventilation, tracer gas

1 | INTRODUCTION

With the rise of awareness of the importance of inhaled air quality and the prevention of cross-contamination, personalized ventilation (PV) has been increasingly gaining the attention of researchers in the past years. PV is a device that provides clean, tempered air into each occupant separately. It aims to improve thermal comfort by providing individual control over the velocity and direction of the supplied flow, thus addressing the different thermal preferences of the users of the room.[1] Besides improving thermal comfort, PV provides a better inhaled indoor air quality compared to total volume systems since it supplies clean air directly to the occupants.[2] PV supplies a flow with low turbulence intensity that is able to penetrate the human convective boundary layer to supply air for inhalation.[3] Thus, PV can enhance the performance of occupants since indoor air quality is proved to have a big influence on productivity.[4] Wargocki et al[5] investigated the influence of contaminants on the performance of office workers; they reported that the subjects made fewer mistakes and were 6.5% more productive under better indoor air quality. Therefore, it is necessary to provide good air quality in office spaces, which can be achieved by implementing PV.[6]

Studies have shown that PV can reduce the risk of infection via airborne viruses and germs in office spaces compared to total volume ventilation.[7] This results in an improved level of employee's health and a decreased number of sick days taken by employees. Hence, the level of productivity is increased by saving lost work days. Moreover, PV increases the satisfaction of the office users with their working environment. Kaczmarczyk et al[8] report that compared to mixing ventilation (MV), the percentage dissatisfied with air quality can considerably drop when PV is used. Moreover, complaints about headaches and decreased ability to thinking clearly were the highest when MV was used. Thus, PV improved the occupants' self-estimated performance.

The literature describes several variations of PV. Desk-mounted PV air diffusers are the most common design of PV in the literature. Melikov et al[9] compared the performance of different PV air terminal devices. Their results indicated that a vertical desk grill supplying clean air upwards into the breathing zone achieved the highest percentage of inhaled PV air. Kaczmarczyk et al[10] also investigated the performance of developed designs of PV air terminals using human subjects to evaluate the acceptability of air quality. They found that a round moveable panel (RMP) that allows adjusting the direction of air and the distance between the panel and the face was the most preferred option. It reportedly provided high inhaled air quality and improved thermal comfort. The positioning of RMP was investigated by Melikov et al[11]; the results showed no significant difference in inhaled air quality when the position of RMP was changed in relation to the manikin's face. However, studies showed that airflow from the front is less likely to cause downdraft sensation.[12,13] The literature reports other possible locations of the PV diffusers that showed promising results in improving the indoor environment. Such design variations include a PV device placed on the desk and coupled with fans,[14] PV nozzles placed on the sides of the workstations supplying opposite jets into the breathing zone,[15] and ceiling-mounted PV.[16]

Although PV is proved to significantly improve the indoor environment, it is still rarely implemented in practice as it requires connecting each desk to the heating, ventilation, and air conditioning (HVAC) system through a duct or a conduit that supplies clean air from the outdoor. While this is easy to achieve in rooms with underfloor air distribution, it constitutes a challenge when PV is used in combination with ventilation systems that implement wall-mounted or ceiling-mounted air supply grills. Moreover, PV requires additional costs related to material, installation, and planning, which makes PV an expensive addition to construction projects. Furthermore, PV can restrict the arrangement of desks, thus limiting the flexibility of the room layout. Therefore, the ductless personalized ventilation (DPV) has been suggested.[17] DPV is a stand-alone flexible system that is independent of the building automation system and requires no extra work during the construction phase. DPV is a desk-mounted system that transports cool fresh air from the lower part of the room and delivers it directly to the occupant's breathing zone. It is used in combination with displacement ventilation (DV) due to the vertical stratification in air temperature and cleanness created by DV. Dalewski et al[18] report that when compared to using DV alone, DPV was able to enhance thermal comfort and the inhaled air quality. Even when the air stratification was disturbed by walking occupants, DPV still improved the inhaled air quality.[19]

Practical Implications

- Personalized ventilation systems can significantly improve the quality of the built environment. Understanding the difference between ducted and ductless systems helps HVAC engineers improve the present air distribution approaches.
- The findings of this study inform occupants about PV and DPV and their implementation in office spaces.

Alsaad and Voelker[20,21] studied the impact of DPV on thermal comfort and air quality; they reported a significant improvement in the built environment when DPV was implemented. Liu et al[22] investigated the resulting indoor environment when combining DPV with radiant floor cooling. Their results showed that DPV can reduce the inhaled air temperature by up to 4.4 K compared to the reference case. Chakroun et al[23] introduced a new variation of DPV named "personalized evaporative cooler" (PEC) that is used in combination with DV and chilled ceilings. PEC sucks the cool air from the lower part of the room and delivers it to the occupants' face after passing it through a pad saturated with water. According to Chakroun et al,[24] PEC in combination with DV supply air temperature at $\theta_s = 24°C$ can achieve the same level of thermal comfort as DV alone with DV supply air temperature at $\theta_s = 21°C$. Mirzai et al[25] report that a flow rate of 10 L/s supplied by PEC can provide acceptable thermal comfort in a room equipped with a chilled ceiling and DV supplying air with a temperature up to 26°C. Further investigations of the performance of PEC under transient conditions showed that the combination of PEC with DV and a chilled ceiling achieved a 7% energy savings compared to the reference cases.[26]

After examining the literature, it was noticed that DPV is not as widely examined as regular ducted PV. Additionally, the performance of DPV and PV systems has been accessed separately with no relation to each other. Therefore, a comparison of both systems directly under the same boundary conditions is necessary to determine the advantages and disadvantages of each system in comparison to the other. The aim is to determine the scenarios where the ductless system can achieve comparable results to those of the ducted system. This offers the opportunity of achieving the high level of indoor air quality and thermal comfort provided by personalized systems without the disadvantages of complexity and extra expenses that are caused by the ductwork required for PV. The performance of DPV and PV was evaluated in this study using steady-state computational fluid dynamics (CFD) simulations; the numerical model was validated first against measured data collected in a climate chamber. Numerical simulations were implemented instead of human subject surveys to allow for direct comparisons between the systems under different boundary conditions without the impact of occupants' individual preferences on the assessment of the systems.

2 | METHODS

2.1 | Computational domain

The numerical configuration of the computational domain corresponds to the set-up utilized in our previously published work[27] to maintain continuity and to allow comparison of the results. DPV and PV were studied in comparison to a reference case in which only DV was present in the room. Thus, three geometries were created: DPV, PV, and no personalized system. All three models consisted of a simulated office geometry with the dimensions of 3 × 3 × 2.44 m, which is the size of the chamber used for the validation (the details of the validation work are presented in Section 2.3). Two occupants were seated at two workstations located at the center of the room; each workstation was equipped with two computer screens and a computer case (Figure 1). The room was ventilated with (DV) using a semi-circular air terminal. The room ceiling held the exhaust outlet and four lighting fixtures. The domain geometry and all its components were arranged in a symmetrical layout around the plane separating the workstations to avoid the influence of the location of the inlet and outlet in relation to each occupant on the assessment of cross-contamination. Detailed properties of the domain are listed in Table 1.

Simulated tracer gases were used to define three contamination sources in the model: contamination from a passive (unheated) source in the room marked with nitrous oxide (N_2O), dermally emitted contamination marked with carbon dioxide (CO_2), and exhaled contamination marked with sulfur hexafluoride (SF_6) (Figure 1). The top of a trash bin located by the wall was modeled as a passive source introducing contamination into the domain. Dermally emitted and exhaled contamination was released from one of the two occupants, who is denoted as the "source occupant" in this study. The groins of the source occupant were generating CO_2 to represent bioeffluents and volatile metabolites from the human body. Moreover, the source occupant continuously exhaled air mixed with SF_6 to simulate infectious expired air. On the other hand, the second occupant was continuously inhaling and was exposed to the three types of pollution. Therefore, s/he is denoted as the "susceptible occupant" in this study. The transient respiratory process was not simulated as this study was conducted under steady-state conditions. The occupants exhaled/inhaled through two nostril openings; the nostril area was equal to 2 × 0.65 cm^2 for each occupant simulating the nostril area of an average person. The nostrils were directed 45° below the horizontal direction with an intervening angle of 30° between the two openings.[29] The exhaled/inhaled velocity at the nostril was 0.77 m/s[30]; the exhaled air temperature was 34°C.[31]

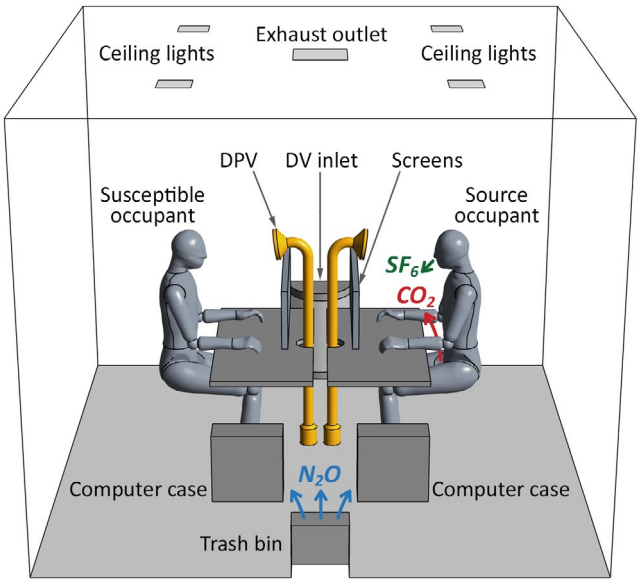

FIGURE 1 The computational domain and the contamination sources of the ductless personalized ventilation (DPV) simulation cases

Ductless personalized ventilation and PV were modeled with a round opening with a diameter of 18 cm (based on the round movable panel [RMP] reported by Kaczmarczyk et al[10]). This large opening is recommended for practical applications in order to cover the range of occupants' slight movements at the desk.[1] The opening of the two personalized systems was located in front of the occupant's face, tilted down from a position slightly above the face corresponding to the opening location preferred by human subjects; the distance between the opening and the occupant's nose was 40 cm.[8,10] DPV was equipped with a round intake opening with a diameter of 10 cm. Since REHVA guidebook reports that the thickness of the first layer of fresh tempered air is 20 cm above the floor when DV is used,[32] DPV intake was located 10 cm above the floor. This also complies with the recommendations of Halvoňová and Melikov.[33]

2.2 | Mesh generation and properties

The mesh was generated using the meshing tool in ANSYS Workbench. To ensure the solution independency of the mesh sizing, a mesh sensitivity study was conducted to determine the association between the mesh size and the numerical results of air velocity, air temperature, and tracer gas concentrations at the center of the domain, at a midpoint between DV and the workstations, and at a midpoint between the trash bin and the workstations. The tested parameters were probed at a height of H = 0.1 m and 1.1 m. These probe points were selected based on their sensitivity to changes in mesh size in test simulations. The independence test simulations were conducted using the geometry of a reference case, that is, without a personalized system. A base case mesh was generated with ~3.75 million unstructured tetrahedral cells with local sizing functions in critical regions and surfaces. Additional five meshing variations were created using the base case mesh sizing settings with a 10% refinement factor to investigate the influence of finer mesh systems on the simulated results.

As illustrated in Figure 2, tracer gas concentrations were more sensitive to the size of the mesh cells compared to air temperature and velocity. The resulting air temperature and velocity only slightly changed when the mesh was refined from ~3.75 to ~6.18 million

TABLE 1 Properties of the simulated reference domain

Component	Dimensions	Heat source	Thermal load[a]
DV inlet	0.4 × 0.5 m (D × H)	Occupants	2 × 70 W
Exhaust outlet	0.3 × 0.3 m	Lighting	4 × 20 W
Lighting fixtures	0.18 × 0.18 m	Computer cases	2 × 75 W
Computer case	0.18 × 0.4 × 0.4 m	Computer screens	4 × 32 W
Computer screen	0.45 × 0.035 × 0.34 m	Total thermal load	498 W
Trash bin	0.3 × 0.15 × 0.3 m	Heat load per unit area	55.3 W/m^2

[a] The power of each heat source is taken from the typical value tables in the ASHRAE standard.[28]

cells. The relative difference in the resulting air temperature at the center of the room (H = 1.1 m) was only 0.1% between the coarsest and finest mesh (Figure 2A). Air velocity exhibited a fairly small relative difference as well (Figure 2B). On the other hand, when probing CO_2 concentration at a midpoint between DV and the workstations at H = 1.1 m, the relative difference was remarkably higher when refining the mesh. The CO_2 concentration increased by 344% when comparing the coarsest and finest mesh, and by only 12% when comparing the finest mesh and its preceding mesh (Figure 2C). Mesh refinement also had an impact on the skewness of the generated mesh. As shown in Figure 2D, the coarse mesh had a higher maximum mesh skewness value of 0.93. This value dropped after the first mesh refinement and stayed more or less unchanged throughout all the cases with finer mesh systems.

As a result, a refined mesh with ~6.18 million cells was adopted in the simulations to capture the tracer gas concentrations as accurately as possible while implementing a reasonable number of mesh cells. Besides the results of the independence test, other factors were considered when generating the final mesh, such as model stability, model convergence, and the balance between good results and reasonable computation time. The adopted mesh was generated with a maximum cell size of 0.06 m. The average $y+$ value for the first layer of cells near the occupants' surface was <1, which is necessary to resolve the wall-bounded turbulent flows at the cell layers next to the surface (where large gradients are expected) without using a wall function for near-wall turbulence modeling.[34,35]

2.3 | Validation of the numerical model

Before conducting the simulations, the numerical model was first validated against empirical measurements. The measurements were conducted in a climate chamber in which an office configuration was set (Figure 3A). A thermal manikin was used to simulate a seated occupant facing a PV outlet. Air velocity, air temperature, and tracer gas (CO_2) concentration were measured at multiple points between the PV outlet and the face; the acquired values were thereafter used to validate the model. The details of the experimental instrumentation are listed in Table 2.

The CFD code ANSYS Fluent was used in this study to solve Reynolds-averaged Navier-Stokes (RANS) equations. Caution was taken to make the geometry of the numerical model as similar as possible to the experimental set-up by carefully measuring configuration in the chamber. Moreover, a 3d-scanned geometry of the manikin in the same sitting posture during the measurements was used in the model since the manikin geometry plays a significant role in simulating the microenvironment around the occupant.[36] The k-ε turbulence model was utilized as it is a robust model that is often implemented for indoor air simulations.[37] Three k-ε models are available: standard (SKE), realizable (RKE), and re-normalization group (RNG); all three models were tested in combination with PRESTO pressure interpolation schemes as this scheme is widely used in the literature. The simulations were conducted using enhanced wall treatment with the incompressible ideal gas law for air density. The second-order upwind discretization scheme was used to solve the

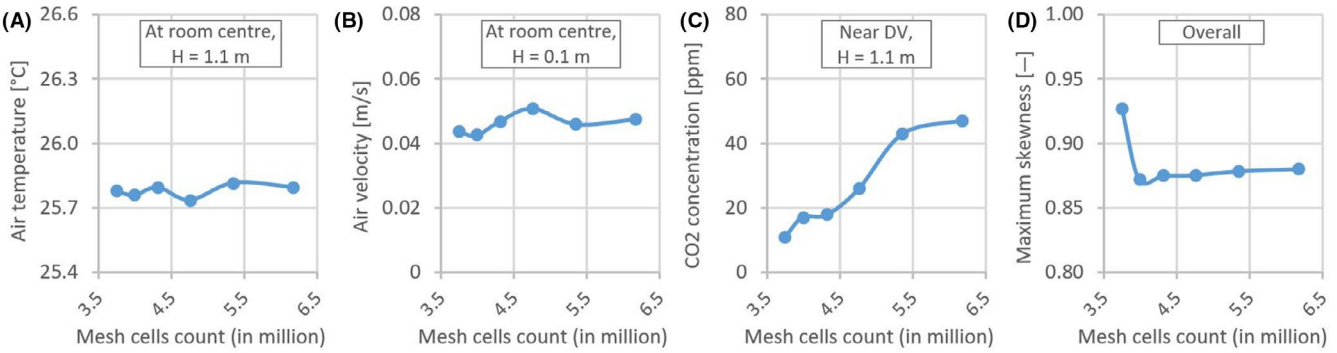

FIGURE 2 Results of the mesh independence test

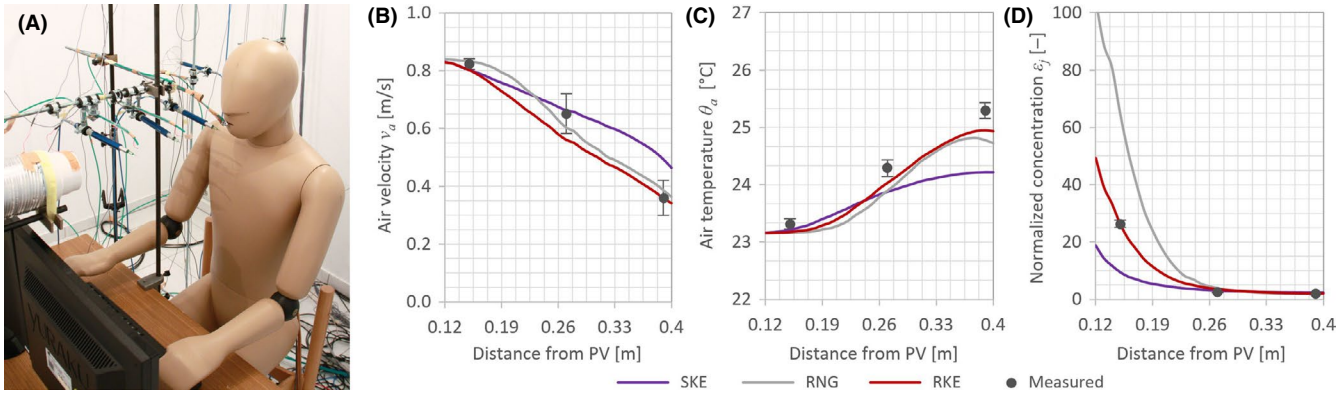

FIGURE 3 (A) The set-up of the validation experiments; (B-D) the measured and simulated air velocity, temperature, and normalized concentration, respectively

TABLE 2 The implemented instrumentation in the validation work

Application	Instrument	Details
Seated occupant	Thermal manikin	Male geometry with 22 body segments 1.76 m tall in the standing position Precision: ±0.2 K
Air temperature	Negative temperature coefficient thermistors	Accuracy: ±0.1 K Resolution: ±0.01 K
Air velocity	Omni-directional hot-wire anemometers	Accuracy: ±1.5% of the measured value Resolution: ±0.001 m/s
Gas concentration	INNOVA1412 photoacoustic gas monitor	Accuracy: ±2% of the measured concentration (for CO_2)

equations of momentum, turbulent kinetic energy and dissipation rate, energy, and species transport.

Figure 3B-D shows the measured and simulated air velocity, air temperature, and normalized concentration, respectively, using the three tested turbulence models. The circles on the graph represent the measurement points. The error bars correspond to the standard deviation of the measurements, which indicates the measured fluctuations over time. The results indicated that the SKE model resulted in the largest disagreement between measured and simulated values. This applies to air velocity, temperature, and tracer gas concentration. The RNG model, on the other hand, achieved the best agreement with the measured air velocity. Yet, it underestimated air temperature and highly overestimated the concentration of tracer gas. The RKE model resulted in the best agreement with all measured parameters. Therefore, it was selected for this study. This outcome agrees with the recommendations in the literature to utilize the RKE model for standard simulation cases because it yields better predictions for spreading rates, flow recirculation, and boundary layers under adverse pressure gradients.[35] Further simulations were conducted to test the validity of the model to simulate inhaled air temperature and velocity under different boundary conditions. Moreover, the influence of other settings on the agreement between measured and simulated data was tested, such as pressure interpolation schemes, the thermal effects and pressure gradient effects associated with enhanced wall treatment, and incorporating the turbulence generation from buoyancy in the dissipation rate equation. Additionally, the S2S radiation model was tested to investigate the impact of the simulation of radiation on the results. It was found that it only had a minor effect on the results while greatly increasing the simulation time, which agrees with the findings of Zhu et al[38] Therefore, radiant heat transfer was not simulated in the model. A full description of the validation work can be found in Alsaad and Voelker.[21]

2.4 | Boundary conditions

As mentioned in Section 2.1, three system variations were compared: DPV, PV, and DV (reference case). Even though PV can improve the indoor environment in both heating and cooling seasons,[39] DPV is designated only for the cooling season since it implements cool air from the lower part of the room supplied by a DV system. Therefore, in this study, the compared systems were evaluated under the environmental parameters of the cooling season. The systems were compared under summer room air temperature (taken at 1.1 m from the floor) of θ_a = 26°C and 29°C. Two room ventilation rates were implemented: $\dot{V}$ = 60 and 75 L/s (n = 10 and 12 h^{-1}) along with two operation modes of the personalized systems: (a) PV (or DPV) switched on at both workstations; (b) PV (or DPV) switched on only at the susceptible workstation while the system is switched off at the source workstation. The second operation mode was only simulated under the room ventilation flow

rate of 75 L/s. Moreover, two airflow rates of the personalized systems were simulated: 10 and 20 L/s. To distinguish the simulation cases from each other when discussing the results, a naming order was implemented consisting of the personalized system name and its flow rate followed by room ventilation rate and ambient temperature. The prefixes "2x" and "1x" were added to the case names to report the operation pattern (at both workstations or only at the susceptible workstation). Thus, the name 2xPV20_60_26 indicates that PV was switched on at both desks with a flow rate of 20 L/s under room ventilation rate of 60 L/s and room air temperature of 26°C. A summary of the simulated variables and boundary conditions is listed in Table 3.

Since outdoor air was delivered into the room only from DV during the DPV cases while it was supplied from the PV diffusers in addition to DV during the PV cases, a direct comparison between the two systems was difficult. To reach a fair comparison between the systems, the amount of air supplied by the displacement ventilation system was reduced when PV was used to keep the total room ventilation airflow (and the air change rate) constant. For example, in the 2xPV20_75_26 case, the implemented PV systems were supplying a total of $\dot{V}_{PV} = 2{\times}20$ L/s of fresh air at the two workstations. Therefore, the flow rate of DV was reduced in this case to $\dot{V}_{DV} = 35$ L/s. Thus, the total ventilation flow rate in the room was $\dot{V} = \dot{V}_{PV} + \dot{V}_{DV} = 75$ L/s in the 2xPV20_75_26 case. To keep the air velocity supplied by the DV system constant, the size of the DV air terminal was reduced during the PV cases to 0.4×0.5 m ($D \times H$).

The same logic was used when defining the temperature of air supplied by PV (θ_{PV}) when comparing PV and DPV. The temperature of air supplied by DPV (θ_{DPV}) depended on air temperature at the DPV intake. Thus, the difference between DPV supplied air temperature and room air temperature was different in each case depending on the difference between room air temperature (at $H = 1.1$ m) and air temperature at the DPV intake level (at $H = 0.1$ m). To avoid the influence of air temperature on tracer gas concentrations, the PV supplied air temperature θ_{PV} was set differently in each case according to the temperature of air supplied by DPV θ_{DPV} in their equivalent cases. This was necessary to maintain an equal air density of the supplied personalized air in the equivalent PV and DPV cases, which ensured similar distribution patterns of the air dispensed by the personalized system diffuser to allow for a direct comparison between the systems based on the source of supplied air.

Furthermore, DPV and PV were defined using different approaches in the model. While PV can be easily defined as a velocity inlet boundary condition, DPV was a challenge. Since the DPV diffuser opening (⌀18 cm) is larger than the air intake (⌀10 cm), adding a momentum source to the cells in the DPV intake resulted in an unequal distribution of supplied air across the opening where fresh supplied air and low air temperature magnitudes are located at the center of the diffuser. Multiple approaches were tested to resolve this issue. One approach was to model a simplified geometry with various shapes and configurations inside the diffuser to control and redirect airflow. Another approach was defining the diffuser as a porous medium. Both approaches failed in generating a uniform air distribution that is comparable to the one supplied by PV. Therefore, the DPV system was modeled by coupling the intake and diffuser as a pair. This means that the air temperature at each surface cell of the DPV diffuser opening is assigned as the area-weighted average of air temperature at the surface cells of the DPV intake. Tracer gas concentration is defined using the same concept. On the other hand, DV was modeled as a velocity inlet and the air exhaust was defined as a pressure outlet with 0 Pa gauge pressure. The occupants were defined as a fixed temperature boundary condition; the occupants' skin temperature was determined using the coupling of CFD and the advanced thermoregulation model developed by Huizenga et al.[40] For the coupling, initial CFD simulations were conducted with a uniform skin temperature of 34°C. Thereafter, the resulted thermal environment around each body segment was manually imported into the thermoregulation model to calculate the skin temperature. Subsequently, the calculated skin temperature for each of the 16 body segments was imported again into the CFD model to conduct the final simulations. Advanced automated coupling such as in Voelker and Alsaad[41] was not used in this study.

TABLE 3 An overview of the simulated parameters and variables

Parameter	Details
Occupants	A source occupant and a susceptible occupant
Simulated pollutants	Exhaled contamination, dermally emitted contamination, and room contamination
Simulated cases	DV (reference case), DPV, and PV
Operation mode	Both occupants switch their systems on Only susceptible occupant switches his/her system on
Personalized flow rate	10 and 20 L/s
Room ventilation rate	60 and 75 L/s
Room air temperature	26 and 29°C
Occupants' surface temperature	Differs in each simulation case based on boundary conditions Determined using the coupling of CFD and thermoregulation
Exhalation/inhalation	Constant with a velocity of 0.77 m/s and air temperature of 34°C

3 | RESULTS

3.1 | Exhaled contamination

As mentioned in Section 2.1, SF_6 was used to mark the exhaled infectious air. Figure 4 shows the inhaled concentration of SF_6 by the susceptible occupant. The inhaled concentration is expressed in the gas mass fraction w_j defined as the ratio of the mass of a certain tracer gas m_j [mg] to the total mass of the gas mixture in the domain m_t [mg] according to:

Thus, the higher the mass fraction, the lower the air quality

$$w_j = \frac{m_j}{m_t} \quad (1)$$

as the concentration of present pollutants is higher. As shown in Figure 4, although PV was expected to significantly improve the inhaled air quality compared to DV reference cases, the 2xPV10 cases only slightly reduced the inhaled SF_6 concentration at the susceptible workstation. This suggests that the PV system at the source workstation was increasing the spread of SF_6 in the room, thus increasing the concentration at the susceptible workstation. Yet, the 2xPV20 cases remarkably improved the inhaled air quality since each PV system was delivering 20 L/s of clean air into the occupied zone. Thus, SF_6 was sufficiently removed from the breathing zone of the susceptible occupant. Interestingly, 2xPV20 cases with room ventilation flow rate $\dot{V}$ = 60 L/s reduced the inhaled SF_6 mass fraction by about 7 times, while the $\dot{V}$ = 75 L/s cases only reduced it by a maximum of 2.4 times during the 2xPV20_75_26 case. Thus, even though more fresh air was delivered into the room during the $\dot{V}$ = 75 L/s cases, it did not lead to the best SF_6 removal due to different air contaminants distribution patterns governed by air velocity fields in the room. As shown in Figure 5, during the $\dot{V}$ = 60 L/s cases, an apparent percentage of SF_6 molecules was pushed away from the workstations toward the floor by the flow supplied by PV. However, during the $\dot{V}$ = 75 L/s case, the larger amount of supplied air by the displacement ventilation system pushed SF_6 molecules up toward the breathing zone, hence resulting in a higher inhaled SF_6 concentration at the susceptible workstation. Additionally, the cases with lower room air set-point temperature (θ_a = 26°C) resulted in a lower inhaled SF_6 mass fraction compared to the cases with θ_a = 29°C. This is because the lower ambient temperature led to a larger difference between the surface temperature of heat sources and the surrounding air. This led to a higher Rayleigh number and subsequently stronger thermal plumes around the heat sources, which increased the removal of pollutants toward the air outlet (located at the center of the ceiling).

Unlike the 2xPV cases, the 2xDPV cases significantly increased the inhaled SF_6 mass fraction at the susceptible workstation. On the contrary to PV cases, increasing the personalized flow rate of DPV increased the inhaled SF_6 concentration at the susceptible workstation even more. During the 60_26 case, the 2xPV20 system configuration achieved an inhaled SF_6 concentration of $w_j = 0.02 \times 10^{-5}$, whereas the 2xDPV20 case resulted in $w_j = 1.42 \times 10^{-5}$. Under the same boundary conditions, 2xPV10 achieved an inhaled concentration of $w_j = 0.12 \times 10^{-5}$, while the 2xDPV10 case achieved $w_j = 0.31 \times 10^{-5}$. Thus, it can be said that at lower personalized flow rates, the performance difference between PV and DPV in removing SF_6 from the inhaled air at the susceptible workstation decreases when PV and DPV were switched on at both workstations.

This changes dramatically when only the susceptible occupant turns on its personalized system. As shown in Figure 6, the 1xDPV10 and 1xPV10 cases achieved fairly comparable inhaled SF_6 concentration. Both systems significantly improved the air quality inhaled by the susceptible occupant compared to the DV reference cases where the inhaled SF_6 concentration was reduced by a maximum of 8 times (achieved during the 1xDPV10_75_26 case). Yet, under a higher personalized flow rate, the ductless system could not compete with the ducted system. The 1xPV20 cases achieved significantly lower inhaled SF_6 mass fraction than the 1xDPV20 cases as the PV20 system was delivering a large amount of fresh air directly into the workstation. The inhaled SF_6 mass fraction at the susceptible workstation was increased by as much as 4.5 times when PV20 was replaced by DPV20 during the 75_26 cases.

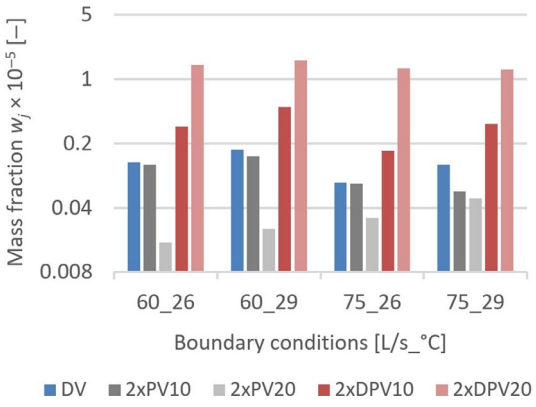

FIGURE 4 Inhaled SF_6 mass fraction at the susceptible workstation when the ductless personalized ventilation (DPV) and personalized ventilation (PV) are switched on at both workstations

3.2 | Dermally emitted contamination

The dermally emitted contaminants from the groins of the source occupant were creating a thick cloud of CO_2 that was mostly concentrated on the source workstation side of the room (Figure 7). CO_2 concentration was high in this cloud as the polluting groins had a relatively large surface area of 161×10^{-4} m^2, emitting CO_2 with a high mass fraction of 5%. A large ratio of this cloud was constrained by the thermal plumes above the computer screens, which removed CO_2 molecules toward the exhaust outlet. Since the supplied flow rate of DV during DPV cases was higher than it was during PV cases, the concentration of CO_2 at the lower part of the room during the DPV cases was smaller than it was during the PV cases. The air jet supplied by DPV and PV infiltrated the CO_2

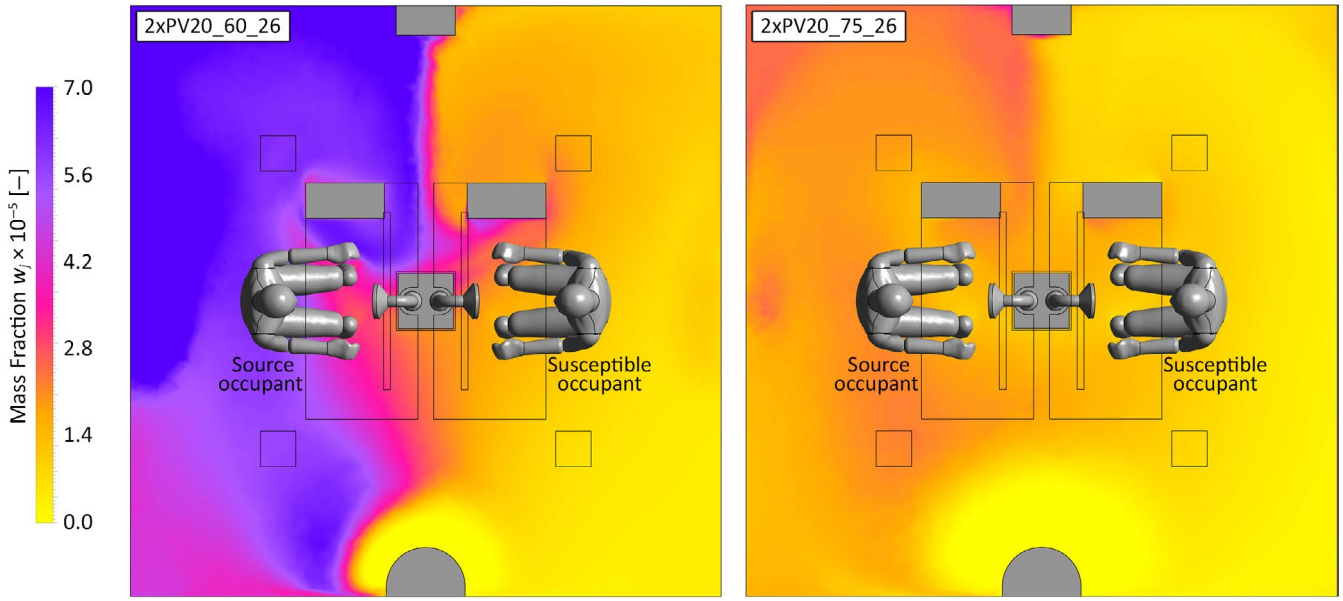

FIGURE 5 The horizontal distribution of SF_6 mass fraction at 10 cm above the floor

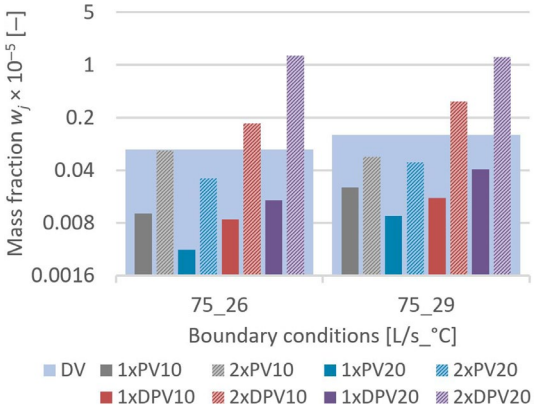

FIGURE 6 Inhaled SF_6 mass fraction at the susceptible workstation

cloud, supplying clean air for inhalation for the source occupant. Figure 8 shows the CO_2 mass fraction inhaled by the source occupant probed at 5 mm from the mouth when the systems were switched on at both workstations. In other words, Figure 8 indicates how much the source occupant was inhaling from the contaminants released from its own groins. The results indicate that both DPV10 and PV10 achieved comparable results in penetrating the CO_2 cloud and improving the inhaled air quality compared to the DV reference cases. PV10 performed slightly better than DPV10 as it supplied 100% clean air, while DPV10 supplied air with a small concentration of CO_2 transported from the DPV10 intake. The highest CO_2 mass fraction inhaled by the source occupant was $w_j = 0.2 \times 10^{-5}$ during the 2xPV10 cases and $w_j = 0.3 \times 10^{-5}$ during the 2xDPV10 cases.

When increasing the velocity of the supplied personalized air, that is, during the PV20 and DPV20 cases, PV significantly improved the inhaled CO_2 concentration at the source workstation. This was because PV20 system was ejecting 20 L/s of clean air into the breathing zone. Additionally, PV10 supplied air with a low velocity; thus, as the personalized air flowed slowly through the CO_2 cloud, it mixed with CO_2 before reaching the targeted inhalation zone, hence reducing the length of the clean air core of the jet. On the other hand, PV20 supplied air at higher velocity through the CO_2 cloud. The CO_2 concentration inhaled by the source occupant was as lower by as much as 6.4 times when switching from 2xPV10 to 2xPV20 during the 60_26 case. Nonetheless, increasing the flow rate of DPV did not have the same influence due to higher mixing with CO_2 molecules at the DPV intake. Compared to the 2xPV20 cases, the 2xDPV20 cases resulted in an inhaled CO_2 mass fraction at the source workstation of 29.6 times higher than the 2xPV20 cases under the 60_26 boundary conditions. Other 2xDPV20 cases resulted in slightly better results.

The resulting inhaled air quality at the susceptible workstation did not indicate the same patterns (Figure 9). Similar to the results of SF_6 diffusion, operating the personalized systems at both desks increased the concentration of the dermally emitted pollution in the room; ergo, lowering inhaled air quality at the susceptible workstation. When the personalized system is switched off at the source workstation, the cross-contamination between the two workstations was lower. The performance of 1xPV10 and 1xDPV10 was highly comparable, with a minor advantage for the 1xPV10 cases (minimum $w_{j,1xPV10} = 0.0168 \times 10^{-5}$; minimum $w_{j,1xDPV10} = 0.0172 \times 10^{-5}$). Increasing the flow rate of the personalized system to 20 L/s exhibited the same patterns reported in the previous section. The higher the flow rate of 1xPV, the lower the CO_2 concentration inhaled by the susceptible occupant. Conversely, the higher the flow rate of 1xDPV, the higher the inhaled CO_2 concentration at the susceptible workstation. Yet, when increasing the flow rate of the systems, the magnitude of performance change is very different between 1xPV and 1xDPV. While switching from

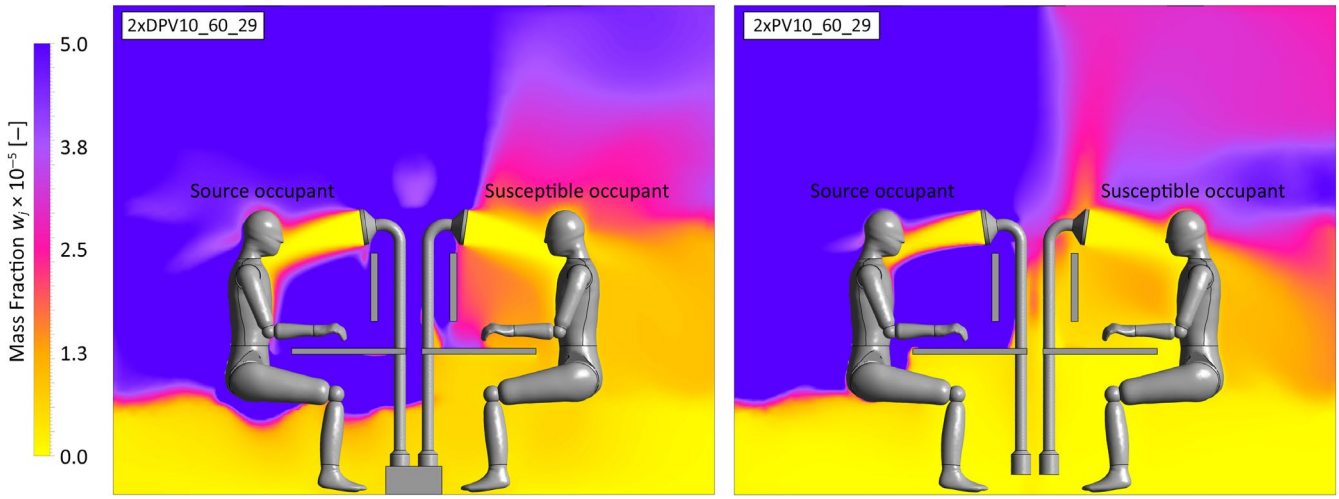

FIGURE 7 Vertical distribution of CO_2 mass fraction in the room

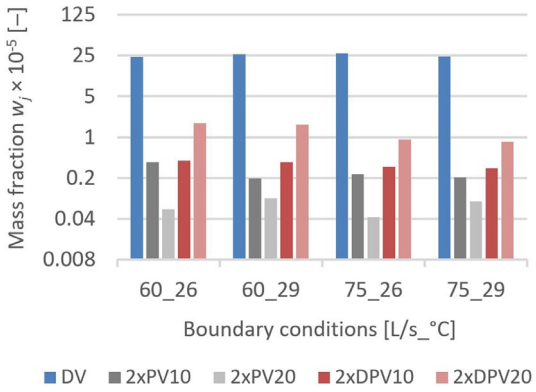

FIGURE 8 Inhaled CO_2 mass fraction at the source workstation when the ductless personalized ventilation (DPV) and personalized ventilation (PV) are switched on at both workstations

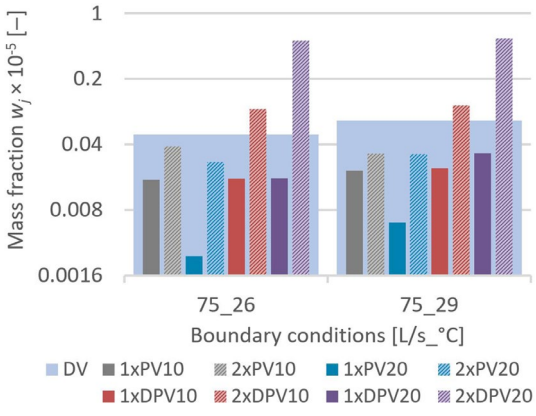

FIGURE 9 Inhaled CO_2 mass fraction at the susceptible workstation

1xDPV10 to 1xDPV20 only slightly affected inhaled CO_2 mass fraction at the susceptible workstation, switching from 1xPV10 to 1xPV20 decreased the inhaled CO_2 concentration by as much as 84.7% during the 75_26 case.

3.3 | Room contamination

The spread of room pollution emitted from the top of a trash bin and marked with N_2O was remarkably different from the human-generated pollution (marked with SF_6 and CO_2). Firstly, the location of the N_2O source in relation to the inhalation zone of the susceptible occupant was different than the location of the SF_6 and CO_2 sources in terms of distance and elevation. Secondly, the human-generated pollution was heated which caused the pollutants to ascend through the thermal plumes. Conversely, the trash bin emitted contamination that flowed in the lower part of the room toward the workstations where the heat sources are located; the buoyancy forces around the computer cases and occupants' bodies then carried the contamination molecules upwards. Therefore, the concentration of N_2O was relatively high at the floor level where the DPV intakes are located. Figure 10 exhibits an isosurface that plots the N_2O mass fraction. It shows that DPV drew N_2O from the floor level and delivered it into the breathing zone. Thus, it increased the inhaled N_2O concentration at the susceptible workstation compared to the DV reference cases. On the other hand, PV supplied clean air that significantly improved the removal of N_2O molecules from the inhaled air.

Figure 11 compares the performance of the systems regarding the inhaled N_2O concentration. It shows that the performance of PV yielded a clear superiority over the performance of DPV in removing room pollution from the inhaled air at the susceptible workstation. During the 2xPV10 cases, the cases with a room ventilation flow rate of $\dot{V}$ = 75 L/s resulted in an inhaled N_2O concentration as low as $w_j = 0.06 \times 10^{-5}$, whereas the cases with $\dot{V}$ = 60 L/s achieved a minimum of $w_j = 0.2 \times 10^{-5}$ due to the less amount of supplied fresh air into the room. These concentrations are remarkably low compared to the inhaled mass fraction achieved by the 2xDPV10 and DV cases, which resulted in a minimum of $w_j = 10.1 \times 10^{-5}$ and 5.7×10^{-5}, respectively. Increasing the personalized flow rate from $\dot{V}_{DPV}$ = 10 L/s to $\dot{V}_{DPV}$ = 20 L/s slightly improved its performance. This can be explained due to the increased momentum at the intakes which led to the mixing

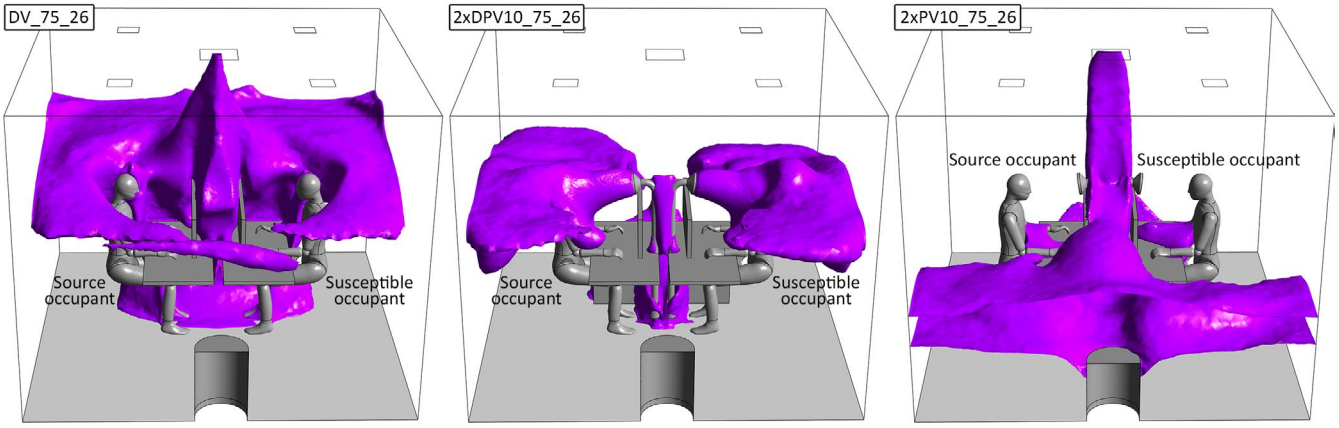

FIGURE 10 N_2O isosurface plotted at $w_j = 6 \times 10^{-5}$ during the 75_26 cases

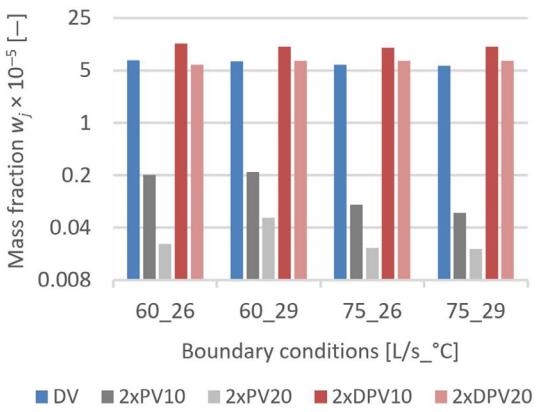

FIGURE 11 Inhaled N_2O mass fraction at the susceptible workstation when the ductless personalized ventilation (DPV) and personalized ventilation (PV) are switched on at both workstations

of high N_2O concentration air at the lower part of the room with low N_2O concentration air above it. Thus, DPV20 was supplying a diluted concentration of N_2O compared to DPV10. On the other hand, increasing the flow rate of PV to 20 L/s notably improved its performance. The inhaled N_2O concentration at the susceptible workstation during the 2xPV20 cases was as low as $w_j = 0.02 \times 10^{-5}$ under the 75_29 boundary conditions. In this case, the N_2O mass fraction inhaled by the susceptible occupant was 321.3 times lower than what it was during the 2xDPV20 case under the same boundary conditions.

Unlike the distribution of exhaled and dermally emitted contaminants, switching the personalized system at the source workstation only marginally impacted the inhaled N_2O concentration at the susceptible workstation. In general, the 2xPV cases achieved a slightly better removal of N_2O compared to the 1xPV cases since the 2xPV cases involved a larger volume of fresh air being supplied into the occupied zone, thus diluting the concentration of N_2O. On the other hand, 1xDPV cases performed better compared to 2xDPV cases since the second DPV system was transporting more N_2O molecules from the floor level to the occupied zone, which increase the concentration of N_2O in this zone.

4 | DISCUSSION

Both PV and DPV aim to deliver clean air into the breathing zone. In the present study, both systems were equipped with the same air terminal device (same size, inclination, distance to the target, and properties of the supplied flow). This led to similar flow interaction patterns at the vicinity of the body. As the susceptible occupant was constantly inhaling air, the inhaled air quality was a result of the flow interaction of mainly two airflows: the free convection flow around the body and the personalized flow from PV and DPV. The invading personalized flow supplied from the front had enough momentum to penetrate the convective flow to supply clean air for inhalation. In the case of the source occupant, a third flow was involved in the flow interaction at the face, namely the two exhaled jets from the nostrils. The exhaled jets flowed through the convective flow during the reference cases and were diffused by the supplied flow during the PV and DPV cases. Detailed information about airflow interaction around the human body can be found in the work of Melikov.[42]

The difference between the two compared systems is the source of the delivered air. In PV cases, the supplied air is 100% clean air drown from the outdoor environment. On the other hand, DPV recirculates the air within the room and moves it from a zone where the contamination concentration is theoretically low into a zone where the contamination concentration is higher. The results discussed above indicate that multiple factors affect the performance of the systems such as the location of the contamination source, the operation mode, the thermal environment, and the supply flow rate. A passive contamination source near the floor level greatly disrupted the performance of DPV. This problem could be resolved by implementing an intake filter to avoid transporting pollutants from the floor level to the breathing zone.[43]

Additionally, the operation pattern of the system played an important role in determining indoor air quality. While turning off the personalized system at the source workstation improved the air quality in the susceptible workstation, turning on the personalized system at both workstations remarkably increased the cross-contamination between the source and susceptible occupants. These results agree with the findings reported by Melikov,[42] who stated

that the personalized flow forces the jets of contaminated exhaled air away for the pollution source; hence, it spreads the contaminants in the occupied zone. PV case simulations showed that the effect of the operation pattern does not only apply for DPV, but to PV as well despite the fact that PV supplies fresh air from the outdoors. The results of this study indicate that turning off PV at the source workstation always mitigated the cross-contamination when contrasted to turning on PV at both workstations. This agrees with the results reported by Shen et al,[44] which indicate that implementing PV by a source person in a room equipped with DV undermines the quality of indoor air in comparison to not having PV. Gilkeson et al[45] also reported that a poorly located PV jet can result in a remarkable decrement in indoor air quality in comparison to the reference case. However, Russo and Khalifa[46] stated that PV does not considerably increase cross-contamination in an office occupied by two users (one with PV and one with no PV). This statement contradicts the findings of Melikov,[42] Shen et al,[44] and the findings of this study. Nevertheless, Russo and Khalifa[46] investigated cross-contamination between two occupants facing two neighboring corners. Thus, PV was pushing the contaminants away from the occupants, unlike the set-up used in this study in which the occupants were facing each over. Additionally, in this study, the power of the computer screens defined in the CFD solver represented the maximum power consumption of a flat-panel screen. This led to a relatively large difference between the screens surface temperature and the room air temperature, consequently leading to a stronger thermal plume that protected the users from cross-contamination when the personalized systems were not used. This accentuated the negative impact of the personalized systems on transporting contaminants between the occupants. Further investigations are required to study the influence of the distribution of thermal plumes and the seating patterns on cross-contamination when PV or DPV is used since the furniture layout is a decisive factor in the distribution of pollutants.[47] Moreover, the location of the contamination sources needs to be further investigated since it plays an important role in the occupants' exposure to contaminants and cross-contamination between occupants.[48]

When switching the personalized system on at the susceptible workstation only, DPV was able to compete with PV in the cases that involved a low personalized flow rate (10 L/s). The setting of the personalized flow rate in real applications is controlled by the users. It is difficult to predict how the users would set the flow as it is tightly connected to individual preferences in addition to other boundary conditions. However, as elevated velocities at the face can cause eye irritation, it is more likely that low personalized flow rates would be implemented which offers a promising possibility of replacing PV with DPV. Another factor should be kept in mind when comparing the two systems, which is the range of applicability. While the air temperature of PV can be controlled through the HVAC system to create a wider range of boundary conditions covering both heating and cooling seasons, DPV is limited to the cooling season in rooms equipped with DV. This makes DPV more suitable for climates with dominant cooling seasons.

5 | CONCLUSIONS AND LIMITATIONS

Two desk-mounted personalized systems were compared in this study: PV and DPV. Results indicated that PV always improved the inhaled air quality and its performance was generally independent of the surrounding indoor environment. When $\dot{V}_{PV} = 10$ L/s, PV only slightly decreased the concentration of exhaled contamination in the inhalation zone of the susceptible occupant when PV was switched on at both workstations. Increasing the flow rate of PV to $\dot{V}_{PV} = 20$ L/s achieved a significantly low SF_6 concentration at the susceptible workstation in comparison to DPV cases in which $\dot{V}_{DPV} = 20$ L/s. Nevertheless, turning off the personalized system at the source workstation improved the performance of DPV and made it even comparable to the performance of PV during the $\dot{V}_{DPV} = 10$ L/s cases. The removal of the dermally emitted contaminants from the susceptible workstation illustrated similar results. DPV was able to compete with PV when the system is switched off at the source workstation and the personalized flow rate is set to $\dot{V}_{DPV} = 10$ L/s. Additionally, both systems achieved good results in supplying clean air into the breathing zone of the source occupant. However, when $\dot{V}_{DPV} = 20$ L/s, the bioeffluents concentration in the inhalation zone of the source occupant during a DPV case was 29.6 times higher than what it was during the equivalent PV case.

The performance of PV yielded a clear superiority over the performance of DPV in removing room contamination emitted from the top of the trash bin. This was a result of PV delivering clean air directly into the breathing zone, while DPV was transporting pollutants from the floor level (where it was highly concentrated) into the breathing zone. Turning off the system at the source workstation slightly improved the performance of DPV in removing room pollution, yet its performance remained far behind the performance of PV.

These conclusions should be considered in light of the limitations that this study encountered. This work involved a large number of numerical simulations. Despite of the extensive validation work, the accuracy of these simulations is limited by the possible numerical errors in the CFD solver and in the thermoregulation model as well. Moreover, human error in obtaining and analyzing data is also possible. An additional limitation of this study was conducting the simulations with a fixed room geometry. As the distribution of thermal plumes and pollution sources in the room play an essential role in the distribution of contamination in the air, it is not possible to draw a decisive conclusion about the performance of DPV in comparison with PV from a single study. Multiple parameters need to be considered in future studies such as room layout, geometry, seating pattern, location of the supply air terminal, location of the exhaust outlet, and the position of pollution sources.

ACKNOWLEDGEMENT

This work was supported by a scholarship from the Deutscher Akademischer Austauschdienst (DAAD) under the Research Grants – Doctoral Programmes in Germany (programme ID: 57129429).

Their constant support is highly appreciated. I would also like to express my gratitude to Prof. Arsen Melikov for his insightful thoughts and recommendations regarding this project during my short research visit at the Technical University of Denmark. We would also like to thank the Digital Bauhaus Lab at the Bauhaus-Universität Weimar for providing the high computational resources required for the CFD simulations. Additionally, we would like to thank the Centre for the Built Environment at the University of California, Berkeley for their cooperation and for facilitating the use of their advanced thermoregulation model. Open access funding enabled and organized by Projekt DEAL.

CONFLICT OF INTEREST

The authors have no conflicts of interest to declare.

AUTHOR CONTRIBUTIONS

Hayder Alsaad: Conceptualization (lead); data curation (lead); formal analysis (lead); funding acquisition (lead); methodology (lead); project administration (lead); validation (lead); writing – original draft (lead); writing – review and editing (equal). **Conrad Voelker:** Funding acquisition (supporting); methodology (supporting); project administration (supporting); supervision (lead); writing – original draft (supporting); writing – review and editing (supporting).

ORCID

Hayder Alsaad https://orcid.org/0000-0001-7738-0193
Conrad Voelker https://orcid.org/0000-0002-3687-0177

REFERENCES

1. Melikov AK. Personalized ventilation. *Indoor Air*. 2004;14:157-167.
2. Melikov AK. Advanced air distribution: improving health and comfort while reducing energy use. *Indoor Air*. 2016;26:112-124.
3. Alsaad H, Voelker C. Qualitative evaluation of the flow supplied by personalized ventilation using schlieren imaging and thermography. *Build Environ*. 2020;167:106450.
4. Tham KW. Indoor air quality and its effects on humans—a review of challenges and developments in the last 30 years. *Energ Build*. 2016;130:637-650.
5. Wargocki P, Wyon DP, Baik YK, Clausen G, Fanger PO. Perceived air quality, sick building syndrome (SBS) symptoms and productivity in an office with two different pollution loads. *Indoor Air*. 1999;9:165-179.
6. Fanger P. Human requirements in future air-conditioned environments. *Int J Refrig*. 2001;24:148-153.
7. Cermak R, Melikov A. Protection of occupants from exhaled infectious agents and floor material emissions in rooms with personalized and underfloor ventilation. *HVAC&R Res*. 2007;13:23-38.
8. Kaczmarczyk J, Melikov A, Fanger PO. Human response to personalized ventilation and mixing ventilation. *Indoor Air*. 2004;14(Suppl 8):17-29.
9. Melikov AK, Cermak R, Majer M. Personalized ventilation: evaluation of different air terminal devices. *Energ Build*. 2002;34:829-836.
10. Kaczmarczyk J, Melikov A, Bolashikov Z, Nikolaev L, Fanger PO. Human response to five designs of personalized ventilation. *HVAC&R Res*. 2006;12:367-384.
11. Melikov AK, Pavlov G, Dimitrov N. Personalized ventilation: impact of airflow direction at the breathing zone on inhaled air quality. *Proceedings of CLIMA 2007 – Wellbeing Indoors, Helsinki, Finland*. 2007.
12. Mayer E, Schwab R. Direction of flow turbulent airflow and thermal comfort. *Proc Healthy Build '88, Stockholm, Sweden*. 1988;2:577-582.
13. Toftum J, Zhou G, Melikov A. *Airflow direction and human sensitivity to draught*. Proceedings of CLIMA 2000, Brussel: REHVA, Paper 336. 1997.
14. Tham KW, Pantelic J. Performance evaluation of the coupling of a desktop personalized ventilation air terminal device and desk mounted fans. *Build Environ*. 2010;45:1941-1950.
15. Zhang H, Arens E, Kim D, Buchberger E, Bauman F, Huizenga C. Comfort, perceived air quality, and work performance in a low-power task–ambient conditioning system. *Build Environ*. 2010;45:29-39.
16. Yang B, Sekhar SC, Melikov AK. Ceiling-mounted personalized ventilation system integrated with a secondary air distribution system – a human response study in hot and humid climate. *Indoor Air*. 2010;20:309-319.
17. Halvoňová B, Melikov AK. "Ductless" personalized ventilation in conjunction with displacement ventilation. *Proceedings of Indoor Air 2008, Copenhagen, Denmark*. 2008.
18. Dalewski M, Melikov AK, Vesely M. Performance of ductless personalized ventilation in conjunction with displacement ventilation: physical environment and human response. *Build Environ*. 2014;81:354-364.
19. Halvoňová B, Melikov AK. Performance of "ductless" personalized ventilation in conjunction with displacement ventilation: Impact of disturbances due to walking person(s). *Build Environ*. 2010;45:427-436.
20. Alsaad H, Voelker C. CFD Assessment of Thermal Comfort and Indoor Air Quality Using Ductless Personalized Ventilation. *Proceedings of the 15th IBPSA Conference, San Francisco, CA, USA*. 2017:113-121.
21. Alsaad H, Voelker C. Performance assessment of a ductless personalized ventilation system using a validated CFD model. *J Build Perform Simul*. 2018;11:689-704.
22. Liu J, Dalgo DA, Zhu S, Li H, Zhang L, Srebric J. Performance analysis of a ductless personalized ventilation combined with radiant floor cooling system and displacement ventilation. *Build Simul*. 2019;12:905-919.
23. Chakroun W, Ghali K, Ghaddar N. IAQ of mixed-air chilled ceiling displacement ventilation system combined with personalized evaporative cooler. *Proceedings of the International Conference on Environmental Pollution and Remediation, Ottawa, Ontario, Canada*. 2011.
24. Chakroun W, Ghaddar N, Ghali K. Chilled ceiling and displacement ventilation aided with personalized evaporative cooler. *Energ Build*. 2011;43:3250-3257.
25. Mirzai S, Ghaddar N, Ghali K, Keblawi A. Design charts for sizing CC/DV system aided with personalized evaporative cooler to the desired thermal comfort. *Energ Build*. 2015;86:203-213.
26. Ghaddar N, Ghali K, Chakroun W. Evaporative cooler improves transient thermal comfort in chilled ceiling displacement ventilation conditioned space. *Energ Build*. 2013;61:51-60.
27. Alsaad H, Voelker C. Performance evaluation of ductless personalized ventilation in comparison with desk fans using numerical simulations. *Indoor Air*. 2020;30:776-789.
28. ASHRAE. *ASHRAE Handbook: Fundamentals*. Atlanta, GA: American Society of Heating, Refrigeration and Air-Conditioning Engineers; 2017.
29. Hyldgård CE. Humans as a source of heat and air pollution. *Proceedings of ROOMVENT '94, Fourth International Conference on Air Distribution in Rooms, Cracow, Poland*. 1994;1:413-433.
30. Bulińska A, Buliński Z. A CFD analysis of different human breathing models and its influence on spatial distribution of indoor air parameters. *Comput Assist Methods Eng Sci*. 2017;22:213-227.
31. Höppe P. Temperatures of expired air under varying climatic conditions. *Int J Biometeorol*. 1981;25:127-132.

32. Skistad H, Mundt E. *Displacement Ventilation in Non-industrial Premises*. Brussels: REHVA, Federation of European Heating and Air-conditioning Associations; 2002.
33. Halvoňová B, Melikov AK. Performance of "ductless" personalized ventilation in conjunction with displacement ventilation: Impact of intake height. *Build Environ*. 2010;45:996-1005.
34. Antoun S, Ghaddar N, Ghali K. Coaxial personalized ventilation system and window performance for human thermal comfort in asymmetrical environment. *Energ Build*. 2016;111:253-266.
35. ANSYS. ANSYS® Academic Research, Release 16.2, Help System, Coupled Field Analysis Guide. 2015. www.ansys.com
36. Topp C, Hesselholt P, Trier M, Nielsen P. Influence of geometry of thermal manikins on concentration distribution and personal exposure. *Proceedings of the 7th International Conference on Healthy Buildings 2003, Singapore*. 2003;2:357-362.
37. Sorensen DN, Nielsen PV. Quality control of computational fluid dynamics in indoor environments. *Indoor Air*. 2003;13:2-17.
38. Zhu S, Cai W, Spengler JD. Control of sleep environment of an infant by wide-cover type personalized ventilation. *Energ Build*. 2016;129:69-80.
39. Kaczmarczyk J, Melikov A, Sliva D. Effect of warm air supplied facially on occupants' comfort. *Build Environ*. 2010;45:848-855.
40. Huizenga C, Zhang H, Arens E. A model of human physiology and comfort for assessing complex thermal environments. *Build Environ*. 2001;36:691-699.
41. Voelker C, Alsaad H. Simulating the human body's microclimate using automatic coupling of CFD and an advanced thermoregulation model. *Indoor Air*. 2018;28:415-425.
42. Melikov AK. Human body micro-environment: the benefits of controlling airflow interaction. *Build Environ*. 2015;91:70-77.
43. Dalewski M, Vesely M, Melikov AK. Ductless personalized ventilation with local air cleaning. *10th International Conference on Healthy Buildings 2012, Brisbane, Australia*. 2012;1.
44. Shen C, Gao N, Wang T. CFD study on the transmission of indoor pollutants under personalized ventilation. *Build Environ*. 2013;63:69-78.
45. Gilkeson N, Khan MA, Noakes C. Computational fluid dynamics simulations of personalised ventilation: the effect of distance and temperature on thermal comfort and air quality. *Proceedings of Roomvent & Ventilation 2018, Espoo, Finland*. 2018:145-150.
46. Russo J, Khalifa HE. Computational study of personal ventilation with multiple occupants and various configurations. *Proceedings of Roomvent 2011, Trondheim, Norway*. 2011.
47. Zhuang R, Li X, Tu J. CFD study of the effects of furniture layout on indoor air quality under typical office ventilation schemes. *Build Simul*. 2014;7:263-275.
48. Pantelic J, Tham KW, Licina D. Effectiveness of a personalized ventilation system in reducing personal exposure against directly released simulated cough droplets. *Indoor Air*. 2015;25:683-693.

How to cite this article: Alsaad H, Voelker C. Could the ductless personalized ventilation be an alternative to the regular ducted personalized ventilation?. *Indoor Air*. 2020;00:1–13. https://doi.org/10.1111/ina.12720